Arabidopsis ABCG34 contributes to defense against necrotrophic pathogens by mediating the secretion of camalexin

Deepa Khare[a], Hyunju Choi[a], Sung Un Huh[b,c], Barbara Bassin[d], Jeongsik Kim[e], Enrico Martinoia[d], Kee Hoon Sohn[a,f], Kyung-Hee Paek[b,1], and Youngsook Lee[a,g,1,2]

[a]Department of Life Sciences, Pohang University of Science and Technology, Pohang 37673, Republic of Korea; [b]Department of Life Sciences, Korea University, Seoul 02841, Republic of Korea; [c]The Sainsbury Laboratory, Norwich NR4 7UH, United Kingdom; [d]Department of Plant and Microbial Biology, University of Zurich, 8008 Zurich, Switzerland; [e]Center for Plant Aging Research, Institute for Basic Science, Daegu 42988, Republic of Korea; [f]School of Interdisciplinary Bioscience and Bioengineering, Pohang University of Science and Technology, Pohang 37673, Republic of Korea; and [g]Division of Integrative Bioscience and Biotechnology, Pohang University of Science and Technology, Pohang 37673, Republic of Korea

Edited by Maarten J. Chrispeels, University of California, San Diego, La Jolla, CA, and approved June 8, 2017 (received for review February 12, 2017)

Plant pathogens cause huge yield losses. Plant defense often depends on toxic secondary metabolites that inhibit pathogen growth. Because most secondary metabolites are also toxic to the plant, specific transporters are needed to deliver them to the pathogens. To identify the transporters that function in plant defense, we screened *Arabidopsis thaliana* mutants of full-size ABCG transporters for hypersensitivity to sclareol, an antifungal compound. We found that *atabcg34* mutants were hypersensitive to sclareol and to the necrotrophic fungi *Alternaria brassicicola* and *Botrytis cinerea*. *AtABCG34* expression was induced by *A. brassicicola* inoculation as well as by methyl-jasmonate, a defense-related phytohormone, and AtABCG34 was polarly localized at the external face of the plasma membrane of epidermal cells of leaves and roots. *atabcg34* mutants secreted less camalexin, a major phytoalexin in *A. thaliana*, whereas plants overexpressing AtABCG34 secreted more camalexin to the leaf surface and were more resistant to the pathogen. When treated with exogenous camalexin, *atabcg34* mutants exhibited hypersensitivity, whereas BY2 cells expressing AtABCG34 exhibited improved resistance. Analyses of natural *Arabidopsis* accessions revealed that AtABCG34 contributes to the disease resistance in naturally occurring genetic variants, albeit to a small extent. Together, our data suggest that AtABCG34 mediates camalexin secretion to the leaf surface and thereby prevents *A. brassicicola* infection.

AtABCG34 | ABC transporters | camalexin | *A. brassicicola* | *B. cinerea*

Plants are exposed to a multitude of pathogens, but they usually resist infection by using their unique defense systems and compounds, including secondary metabolites produced either constitutively (phytoanticipins) or in response to pathogen attack (phytoalexins). Plants produce tens of thousands of secondary metabolites, which are classified as phenolics, terpenoids, alkaloids, glucosinolates, cyanogenic glucosides, and betanins. Secondary metabolites are secreted from the infected cells and their surrounding cells after pathogen attack or are released, hydrolyzed, and become toxic when the cells are destroyed by pathogens (1), thus inhibiting pathogen growth on the plant. Many secondary metabolites are dangerous to the plants because of their toxicity to cellular metabolism. To avoid self-toxicity, plants either secrete these compounds to the leaf surface or sequester them in the vacuole, a compartment with low metabolic activity. In both cases, specific transporters are required either to deliver the secondary metabolites to the site where the pathogens are located or to store them as weapons against pathogen attack.

Several full-size ABCG transporters are involved in the transport of secondary metabolites. *Nicotiana plumbaginifolia* PDR1/ABC1 and *Nicotiana tabacum* PDR1 are induced by jasmonate, a defense-related hormone highly expressed in the leaf epidermal cells and trichomes, and transport sclareol, a diterpene alcohol secreted by *Nicotiana* species in response to pathogen attack (2–4). Two functionally redundant *Nicotiana benthamiana* full-size ABCG transporters, NbABCG1 and NbABCG2, are essential for resistance to *Phytophthora infestans*. Mutants with defects in these two ABCG transporters export much less capsidiol than do the corresponding wild-type plants, indicating that these transporters transport capsidiol (5). NtABCG5/NtPDR5 is induced by insect herbivory, and the absence of this transporter decreases resistance to insects, indicating that it is involved in the transport of a hitherto unidentified insecticidal compound (6). Absence of PhPDR2 increases insect herbivory in *Petunia hybrida* leaves and decreases concentrations of the insecticidal steroid petuniasterone (7). CrTPT2, expressed at the plasma membrane of *Catharanthus roseus*, secretes catharanthine to the leaf surface (8). Lr34, an ABCG transporter in *Triticum aestivum* (wheat), is one of the few durable resistance genes that protect the plant from multiple pathogens, namely *Puccinia triticina* and *Puccinia striiformis*, which cause leaf rust, and *Blumeria graminis*, which causes powdery mildew (9). Furthermore, when heterologously expressed in *Oryza sativa* (rice), Lr34 confers resistance to multiple isolates of *Magnaporthe oryzae* (10) and therefore is a promising candidate ABC transporter to improve crop plants' resistance to a broad spectrum of pathogens. However, the substrate transported by Lr34 is still unknown.

Significance

***Alternaria brassicicola* infection causes dark spots on the leaves of most *Brassica* species, reducing the yield of economically important oilseed crops. In response to *A. brassicicola* infection, *Arabidopsis thaliana* and other Brassicaceae produce and secrete camalexin, a major phytoalexin imparting resistance to *A. brassicicola*. Because camalexin is toxic to the plant itself, specific transporters are needed for secretion. Here we show that the ABC transporter ABCG34 mediates the secretion of camalexin from the epidermal cells to the surface of leaves and thereby confers resistance to *A. brassicicola* infection. This work establishes a complete picture of a plant defense system, consisting of a toxic secondary metabolite, its transporter, and the disease phenotype caused by an economically important pathogen.**

Author contributions: D.K., H.C., S.U.H., E.M., K.H.S., K.-H.P., and Y.L. designed research; D.K., H.C., S.U.H., and B.B. performed research; D.K. and J.K. analyzed data; and D.K., E.M., K.H.S., K.-H.P., and Y.L. wrote the paper.

The authors declare no conflict of interest.

This article is a PNAS Direct Submission.

[1]K.-H.P. and Y.L. contributed equally to this work.

[2]To whom correspondence should be addressed. Email: ylee@postech.ac.kr.

This article contains supporting information online at www.pnas.org/lookup/suppl/doi:10.1073/pnas.1702259114/-/DCSupplemental.

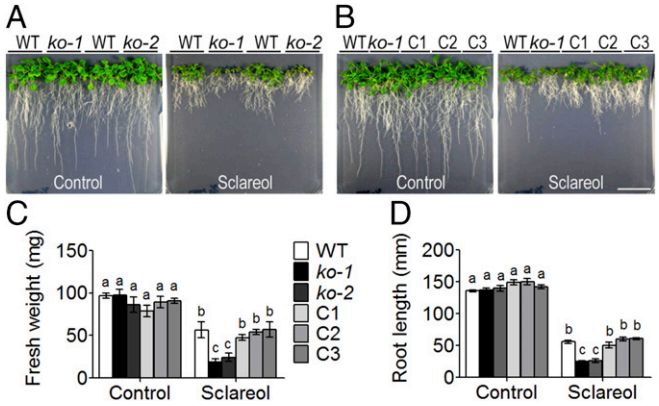

Fig. 1. Sclareol-sensitive phenotype of *atabcg34*-knockout plants. (*A*) *atabcg34* mutants (*ko-1* and *ko-2*) exhibit enhanced sclareol sensitivity compared with the wild-type plants. Plants were grown on 1/2MS-agar plates in the absence (Control) or presence of 65 μM sclareol for 2 wk. (*B*) Sclareol tolerance was restored in complementation lines (C1–C3) expressing $ABCG34_{pro}$*:sGFP:ABCG34* in the *ko-1* background. Plants were grown on 1/2MS-agar plates without (Control) or with supplementation of 65 μM sclareol for 2 wk. (Scale bar, 1 cm.) (*C* and *D*) Plant growth quantified by measuring fresh weight (*C*) and the longest root length (*D*) of 2-wk-old plants. Results are mean values (±SE) of three independent experiments with three replicates each. Different lowercase letters indicate that the means are significantly different between genotypes or treatments [Tukey's honestly significant difference (HSD) test; $P < 0.01$; $n = 3$].

Among the 129 ABC proteins present in *Arabidopsis thaliana*, only two have been implicated in the defense response. PDR8/ABCG36/PEN3, which is localized at the plasma membrane, recruited to infection sites (11), and involved in glucosinolate-dependent pathogen defense at the contact site (12), blocks the penetration of nonhost fungal pathogens (13). Recently, a report suggested that this protein transports 4-O-β-D-glucosyl-indol-3-yl formamide (4OGlcI3F) (14); however, this possibility remains to be proven. *atabcg40/pdr12* mutants exhibit sensitivity to sclareol, and *AtABCG40/PDR12* is induced by pathogen inoculation (15). However, sclareol is not likely to be the natural substrate of AtABCG40, because it is not synthesized in *A. thaliana*. Thus, AtABCG40 might transport chemicals similar to sclareol that are produced by *A. thaliana* in response to pathogen attack.

We hypothesized that additional ABCG transporters are involved in pathogen defense, because (*i*) the transcript levels of many additional full-size ABCG transporters have been reported to be up-regulated in plants exposed to pathogens (16, 17) and (*ii*) pathogen defense is often mediated by secondary metabolites, many of which are transported by ABC transporters (18). To identify such additional ABCG transporters involved in plant defense against pathogens, we screened *A. thaliana* transfer DNA (T-DNA) insertion mutants of full-size *ABCG* genes for altered sensitivity to the secondary metabolite sclareol, because sclareol hypersensitivity might provide a clue as to which ABCG proteins are involved in secondary metabolite transport. Having established that *atabcg34* is hypersensitive to sclareol, we analyzed the function of AtABCG34 in relation to the transport of secondary metabolites implicated in pathogen defense.

Results

***atabcg34* Mutants Exhibit Hypersensitivity to Sclareol.** To identify additional transporters involved in pathogen defense, we exposed 13 of the 15 full-length *A. thaliana abcg* transporter mutants (knockout mutants of *atabcg42* and *atabcg43* were not available at the time of screening) to a toxic concentration of sclareol (65 μM). Among the mutants, *atabcg34-1* (*ko-1*; SAIL_5_G10) and *atabcg34-2* (*ko-2*; SALK_036087) (Fig. S1) exhibited the strongest reduction in both fresh weight and root length in sclareol-containing medium (Fig. 1 *A*, *C*, and *D*). Expression of the genomic fragment of *AtABCG34* ($ABCG34_{pro}$*:sGFP:ABCG34*; genomic DNA) rescued the mutants from sensitivity to sclareol; both fresh weight and root length of the complementation lines recovered to levels similar to those of wild-type plants in half-strength Murashige–Skoog (1/2MS) medium supplemented with 65 μM sclareol (see Fig. 1 *B–D* for *ko-1* and Fig. S2 for *ko-2*). Interestingly, although AtABCG39 is the closest relative of AtABCG34 among the full-size ABCG members (Fig. S3*A*), and its amino acid sequence is 89% identical with that of AtABCG34, the *atabcg39* mutant was not sensitive to sclareol (Fig. S3 *B* and *C*).

AtABCG34 Contributes to Plant Defense Against Necrotrophic Fungi. Because sclareol is known to restrict fungal growth (19, 20), we speculated that AtABCG34 might be involved in defense against fungal pathogens. We evaluated this possibility by inoculating the *atabcg34* mutants (*ko-1* and *ko-2*) with two different necrotrophic fungi, *Botrytis cinerea* and *Alternaria brassicicola*. Although the wild-type leaves inoculated with the two pathogens became necrotic only at the inoculation sites, the mutant leaves exhibited much more extensive necrotic areas upon infection with *A. brassicicola* (Fig. 2 *A* and *B*) or *B. cinerea* (Fig. S4*A*, *Left*), suggesting that the mutants were hypersensitive to both necrotrophic fungal pathogens. Quantification of the pathogen growth confirmed that the *atabcg34* mutants were hypersensitive to the fungal pathogens. *A. brassicicola* growth, quantified using qPCR of *A. brassicicola cutinase A* genomic DNA relative to *A. thaliana α-shaggy kinase* genomic DNA, was higher in the mutant leaves than in leaves of the wild-type plants or the complementation lines (Fig. 2*C*). *B. cinerea* growth, measured by counting spore numbers (Fig. S4*A*, *Right*), was also higher in the mutant leaves than in the wild-type leaves. By contrast, the mutants' response to a bacterial pathogen *Pseudomonas syringae pv. tomato* DC3000 (*Pst* DC3000) was similar to that of the wild-type plants (Fig. S4*B*). Furthermore, expression of the genomic fragment of *AtABCG34* ($ABCG34_{pro}$*:sGFP:ABCG34*; genomic DNA) rescued the mutants from sensitivity to *A. brassicicola* (Fig. 2).

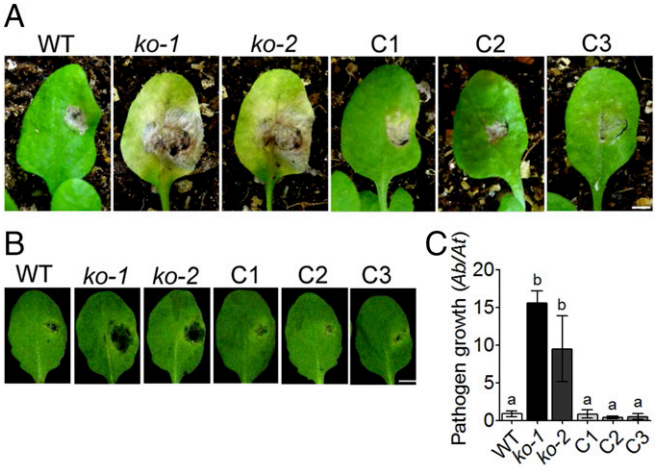

Fig. 2. AtABCG34 is required for resistance to *A. brassicicola*. (*A* and *B*) Disease symptoms of *atabcg34* mutants (*ko-1* and *ko-2*) and complementation lines (C1–C3) on intact plants at 2 wk postinoculation (*A*) and on detached leaves 5 dpi (*B*). (Scale bar, 5 mm.) (*C*) Fungal growth, as determined by amplification of the *A. brassicicola cutinase* A (*Ab*) gene relative to the *A. thaliana α shaggy kinase* (*At*) gene by qPCR at 5 dpi with *A. brassicicola* (5×10^5 spores/mL). The graph represents mean values (±SE) of three biological replicates with at least 21 disease lesions. Different lowercase letters indicate that the means are significantly different between the genotypes (Tukey's HSD test, $P < 0.01$; $n = 3$).

***AtABCG34* Expression Is Induced by Methyl Jasmonate and Necrotrophic Pathogens.** We then analyzed whether the expression level of *AtABCG34* changes in response to treatment with either methyl jasmonate (MeJA) or salicylic acid (SA), hormones that are known to function in the pathogen-defense response. *AtABCG34* expression was induced up to sevenfold within 1 h of MeJA treatment (Fig. 3*A*) but was only slightly induced by SA treatment (Fig. 3*B*). Next, we analyzed the transcript levels of *AtABCG34* in plants exposed to necrotrophic fungi (*A. brassicicola* and *B. cinerea*). *AtABCG34* transcript levels increased three- to sixfold in a time-dependent manner in response to treatment with necrotrophic fungal pathogens (Fig. 3*C* and Fig. S5*A*).

β-Glucuronidase (GUS) staining of $ABCG34_{pro}$*:GUS* lines at 3 d postinoculation (dpi) also revealed the high expression of *AtABCG34* around the *B. cinerea* infection sites (Fig. S5*B*). Thus, *AtABCG34* expression was strongly induced by necrotrophic fungal pathogens (*A. brassicicola* and *B. cinerea*) and by MeJA but not by SA.

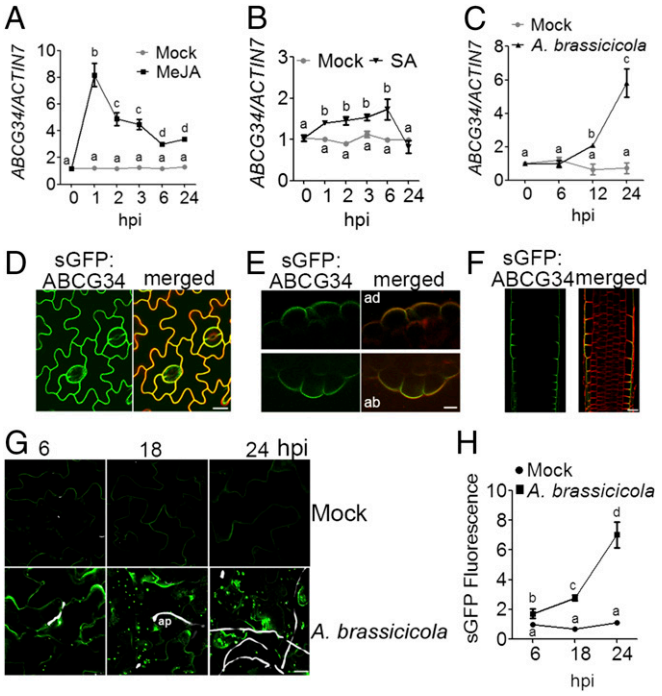

Fig. 3. Expression profile after treatment with MeJA, SA, and *A. brassicicola* and polar localization of AtABCG34. (*A–C*) Time-dependent changes in the transcript level of *AtABCG34* in mature leaves treated with 50 μM MeJA (*A*), 1 mM SA (*B*), or *A. brassicicola* (5×10^5 spores/mL) (C), quantified relative to that of *AtACTIN7*. Data represent mean values (±SE) of three independent experiments. Different lowercase letters indicate that the means are significantly different (Tukey's HSD test, $P < 0.01$; $n = 3$). (*D*) Plasma membrane localization of $ABCG34_{pro}$*:sGFP:ABCG34* expressed in the *ko-1* mutant at the epidermal cells of the mature rosette leaves. The images were taken at a higher gain than the images in *G*. (*E* and *F*) Polar localization of sGFP:ABCG34 in transverse sections of mature leaf at the adaxial (*Upper*) and abaxial (*Lower*) surface (*E*) and root (*F*). FM4-64 (10 μM) was used as a plasma membrane marker. (Scale bars in *D–F*, 10 μm.) (*G* and *H*) Increase in GFP fluorescence of $ABCG34_{pro}$*:sGFP:ABCG34*-expression in the epidermal cells of leaves inoculated with *A. brassicicola* (5×10^5 spores/mL) observed at 6, 18, and 24 hpi (*G*). (Scale bar, 70 μm.) Fungal hyphae (white) were stained with Calcofluor white stain. ap, appressorium. In *H*, sGFP fluorescence intensity was quantified and normalized to that from mock-treated cells at 6 hpi, which was set to 1, using ImageJ, from photographs as shown in *G*. Different lowercase letters indicate that the means are significantly different (Tukey's HSD test, $P < 0.05$; $n = 10$).

AtABCG34 Displays Polar Localization at the Outer Surface of the Plasma Membrane of Epidermal Cells. Next, we examined the subcellular localization of AtABCG34 in complementation lines expressing $ABCG34_{pro}$*:sGFP:ABCG34* in the *atabcg34-1* background. The leaves of the transgenic plants were stained with FM4-64 for only 10 min on ice to prevent the dye from entering the cells. Under this condition, the red fluorescence of FM4-64 delineated only the plasma membrane, and the green fluorescence of sGFP-ABCG34 was colocalized with the red fluorescence (Fig. 3*D*), suggesting that AtABCG34 is localized to the plasma membrane. Interestingly, observation of the transverse sections of the leaves revealed that AtABCG34 was polarly localized at the outer half of the epidermal cells at both the adaxial and the abaxial surfaces (Fig. 3*E*). A similar pattern of polar localization at the outer surface of the epidermal cells was observed in the root (Fig. 3*F*).

To determine whether pathogens affect AtABCG34 localization, we observed synthetic GFP (sGFP) fluorescence in leaves expressing $ABCG34_{pro}$*:sGFP:ABCG34* in the *atabcg34-1* background. When treated with *A. brassicicola*, the green fluorescence of sGFP:ABCG34 increased continuously until 24 h postinoculation (hpi) (Fig. 3 *G* and *H*), indicating induction of AtABCG34 by the pathogen, in agreement with the results of our qRT-PCR analysis (Fig. 3*C* and Fig. S5*A*) and GUS expression assay (Fig. S5*B*). Interestingly, in contrast to nontreated plants, the fluorescence was localized not only at the plasma membrane but also in dot-like structures in the cells (Fig. 3*G*).

***atabcg34* Exhibits Reduced Camalexin Abundance at the Leaf Surface.** The polar localization of AtABCG34 at the plasma membrane and hypersensitivity of *atabcg34* to necrotrophic pathogens suggest that AtABCG34 may be required for the secretion of chemicals that protect plants from pathogen attack. Two different classes of such chemicals may be involved in this process: surface-coating materials, as shown for AtABCG32/PEC1 (21, 22), and secondary metabolites, as shown for AtABCG36/PDR8/PEN3 (14). We tested the first possibility by an ethanol penetration assay that detects permeability defects but could not observe any difference in ethanol penetration between the wild-type plants and *atabcg34* mutants (Fig. S6*A*).

To test the second possibility, that AtABCG34 mediates the secretion of secondary metabolites, we compared the levels of some secondary metabolites in the wild-type plants and the *atabcg34* mutants. The levels and the kinds of phenolic compounds in plants infected with *B. cinerea* did not differ between the *atabcg34* mutants and wild-type plants (Fig. S6*B*). Furthermore, there was no distinct difference in glucosinolate content in plants infected by *A. brassicicola* (Fig. S6*C*). Camalexin is a major phytoalexin produced by *A. thaliana* and other Brassicaceae and is known to be induced by *A. brassicicola* infection and to be required for resistance against *A. brassicicola* (23). Consequently, we determined the camalexin contents at the surface of whole rosettes and observed that it was reduced to about half in *atabcg34* mutants compared with the wild-type plants at both 24 (Fig. 4*A*) and 48 hpi (Fig. S6*D*) with *A. brassicicola*. At 24 hpi the camalexin levels at the rosette leaf surface in the complementation lines were similar to those in the wild-type plants (Fig. 4*A*). The total camalexin content of the whole rosette of *atabcg34* mutants was also reduced compared with that of the wild-type plants at 24 and 48 hpi with *A. brassicicola* (Fig. 4*B*). These data suggest that AtABCG34 is necessary for camalexin secretion to the surface upon *A. brassicicola* infection.

We further tested this possibility by generating *AtABCG34* overexpression lines in the wild-type background. The rosette leaves of plants expressing $35S_{pro}$*:sGFP:ABCG34* (OE1–OE3) exhibited higher levels of surface camalexin at 24 hpi than did the wild-type rosette leaves (Fig. 4*A*). The increased secretion of camalexin was accompanied by improved disease resistance to

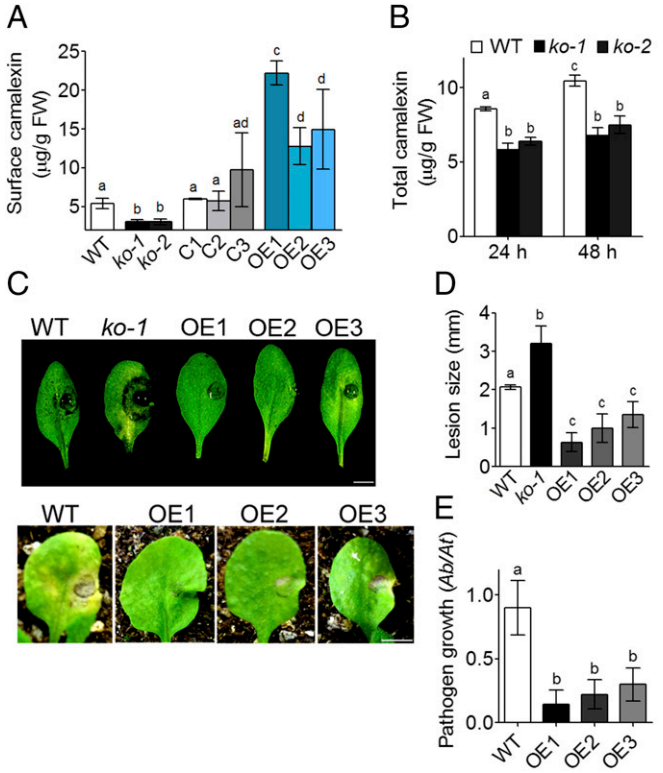

Fig. 4. AtABCG34 mediates the secretion of camalexin to the leaf surface. (*A*) Surface camalexin measured from whole rosettes of wild-type plants, *atabcg34* lines (*ko-1* and *ko-2*), complementation lines (C1–C3), and overexpression lines (OE1–OE3) expressing $35S_{pro}$*:sGFP:ABCG34* in the wild-type background at 24 hpi of *A. brassicicola* (5×10^5 spores/mL). The graph represents mean values (±SE) from five different experiments with at least six rosettes per genotype per experiment. Different lowercase letters indicate that the means are significantly different between genotypes (Tukey's HSD test, $P < 0.01$; $n = 5$). (*B*) Total camalexin measured from whole rosettes of wild-type *A. thaliana* and *atabcg34* (*ko-1* and *ko-2*) mutants at 24 hpi of *A. brassicicola*. Graphs represent mean values (±SE) from five different experiments with at least six rosettes per genotype for each time point in each experiment. Different lowercase letters indicate that the means are significantly different between genotypes or time points (Tukey's HSD test, $P < 0.01$; $n = 5$). (*C*) Photographs of disease symptoms of wild-type plants, *atabcg34-1* mutants, and AtABCG34-overexpressing lines (OE1–OE3) on detached leaves (*Upper*) and intact plants (*Lower*) taken at 3 and 14 dpi of *A. brassicicola*, respectively. (Scale bar, 5 mm.) (*D* and *E*) Lesion diameter ($n = 3$) (*D*) and *A. brassicicola* growth quantified by amplification of the *A. brassicicola cutinase* A (*Ab*) gene relative to the *A. thaliana* α *shaggy kinase* (*At*) gene by qPCR ($n = 3$) (*E*). Graphs represent mean values (±SE) from three biological experiments with at least 15 leaves per genotype and experiment. Different lowercase letters indicate that the means are significantly different between genotypes (Tukey's HSD test, $P < 0.01$).

A. brassicicola (Fig. 4 *C–E*): Lesion diameter and pathogen growth were significantly reduced in all three overexpression lines treated with this pathogen compared with the wild-type plants (Fig. 4 *D* and *E*).

AtABCG34 Expression Improves Tolerance to Camalexin in *A. thaliana* and BY2 Cells. Because camalexin is known to be toxic to *A. thaliana* cells in suspension cultures (24), we next compared the effect of exogenously applied camalexin on the mature leaf surface of wild-type plants and *atabcg34* mutants. Cell death induced by camalexin treatment was analyzed by Evans blue staining. The leaves of both *atabcg34* mutants exhibited significantly higher rates of cell death in response to camalexin treatment than did the wild-type plants and the complementation lines. However, the cell-death response in the leaves of the *atpad3-1* mutant, which has a point mutation in the gene encoding a key enzyme in camalexin biosynthesis and exhibits susceptibility to *A. brassicicola* (25), did not differ from that of the wild-type plants or the complementation lines following camalexin treatment (Fig. 5*A*, *Middle*). By contrast, *atabcg34* and *atpad3-1* mutants were similar in their responses to *A. brassicicola* treatment, exhibiting significantly increased levels of cell death compared with the wild-type plants and the complementation lines (Fig. 5*A*, *Bottom*).

We then tested whether AtABCG34 can confer camalexin tolerance in a heterologous system. For this purpose, we expressed $35S_{pro}$*:sGFP:ABCG34* [coding DNA sequence (CDS)] in tobacco Bright Yellow 2 (BY2) cells. AtABCG34 was localized at the plasma membrane in BY2 cells (Fig. 5*B*, *Middle* and *Bottom*), similarly as in *A. thaliana* cells (Fig. 3*D*), by contrast to the cytosolic localization of free sGFP [empty vector (EV)] (Fig. 5*B*, *Top*). When cultured in medium containing camalexin, AtABCG34-expressing BY2 cells (ABCG34-1 and ABCG34-2) exhibited reduced rates of cell death (Fig. 5*C*) and increased cell density (Fig. 5*D*) compared with the EV-expressing cells.

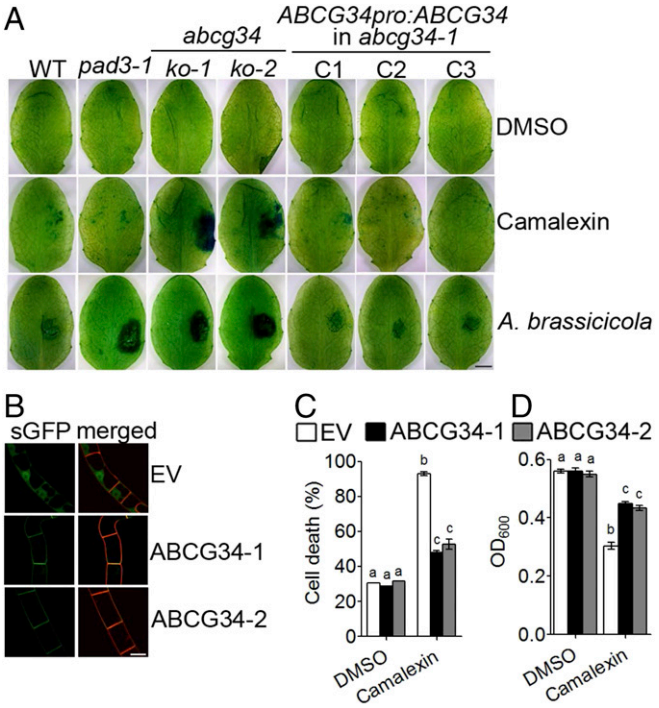

Fig. 5. Camalexin toxicity assay in *A. thaliana* and BY2 cells. (*A*) Photographs of cell death in 3- to 4-wk-old plants using Evans blue staining 24 h after treatment with DMSO (1%) (*Top*), camalexin (1 mg/mL) (*Middle*), or *A. brassicicola* (5×10^5 spores/mL) (*Bottom*). The experiment was repeated four independent times with similar results ($n = 4$). (Scale bar, 5 mm.) (*B*) BY2 cells expressing $35S_{pro}$*:sGFP* empty vector (EV) (*Top*) and $35S_{pro}$*:sGFP:ABCG34* (ABCG34-1 and ABCG34-2) (*Middle* and *Bottom*, respectively). Merged indicates colocalization with red fluorescence of FM4-64 (10 μM), a plasma membrane marker. (Scale bar, 20 μm.) (*C*) Camalexin-induced cell death in BY2 cells expressing EV or AtABCG34. A 6-d-old culture of BY2 cells was treated with either DMSO (0.05%) or camalexin (250 μM), and cell death was analyzed by Evans blue staining 24 h after treatment. (*D*) Camalexin-induced growth inhibition of BY2 cells. A 3-d-old culture of BY2 cells was treated with either DMSO (0.01%) or camalexin (50 μM), and 4 d after treatment the OD at 600 nm was measured. Graphs in *C* and *D* represent mean values (±SE) of three independent experiments. Different lowercase letters indicate that the means are significantly different (Tukey's HSD test, $P < 0.01$; $n = 3$).

AtABCG34 Contributes to Preinvasion Resistance Against *A. brassicicola*. Plants exhibit a multilayered defense response to *A. brassicicola* that is composed of pre- and postinvasion stages. Formation of an appressorium, a swollen structure at the tip of growing hyphae that penetrates the plant cell wall (26), marks the preinvasion stage. Under our experimental conditions, appressoria were observed at 18 hpi with *A. brassicicola* (Fig. 3*G*), consistent with a previous report that appressoria formed at 12–24 hpi with *A. brassicicola* (27). Because *AtABCG34* expression induced by *A. brassicicola* treatment was apparent at 12 hpi (Fig. 3 *C* and *H*), a relatively early time point during the pathogen-defense response (i.e., before appressorium formation), we suspected that AtABCG34 might contribute to resistance at the preinvasion stage. We tested this possibility using three different methods. First, we counted the pathogen penetration sites by callose staining in the wild-type plants, *atabcg34* mutants, and complementation lines. Callose is deposited at the penetration site in response to *A. brassicicola* treatment (28), and a high number of callose depositions indicates a failure to overcome the pathogen at the preinvasion stage (5, 29). *atabcg34* mutants exhibited a significantly higher number of penetration sites than did the wild-type and complementation lines (Fig. 6 *A* and *B*). We also analyzed the *atpad3-1* mutant and found that it exhibited a high penetration frequency similar to that of the *atabcg34* mutants (Fig. 6 *A* and *B*). These results support the notion that the reduction of camalexin content/secretion compromised defense against *A. brassicicola* at the preinvasion stage. Second, we examined the *A. brassicicola* conidia germination in the wild-type and AtABCG34 over-expressing lines. We found that overexpression lines exhibited significantly lower rates of conidia germination than did the wild-type plants (Fig. 6*C*), indicating that AtABCG34 plays an important role in preventing the conidia germination before invasion to the leaf. Third, we tested whether *PDF1.2* induction by pathogens differs between the wild-type plants and the mutants. *PDF1.2* is induced by *A. brassicicola* infection and plays an important role in the preinvasion stage of resistance (30). *PDF1.2* expression increased in both the wild-type and the mutants inoculated with *A. brassicicola* or *B. cinerea*, but the extent of the increase was significantly less in *atabcg34* mutants than in the wild-type plants (Fig. 6*D*).

Accessions Assay to Evaluate the Contribution of AtABCG34 to Resistance Against *A. brassicicola*. Next, we asked whether AtABCG34 is an important factor in determining the defense response to *A. brassicicola* among natural *Arabidopsis* accessions. To address this question, we used *Arabidopsis* accessions that were reported to exhibit different levels of resistance to *A. brassicicola* infection (31): Dijon-G and C24 as susceptible phenotypes; Aua/Rhon (Aa), Cape Verde (Cvi), RLD-1, and Columbia-0 (Col-0) as phenotypes with intermediate resistance; and Kendallville, Muehlen (Mh), Ksk-1, Turk Lake (Tul-0), Bensheim (Be-0), and Nossen (No-0) as resistant phenotypes. We evaluated the different accessions for their *AtABCG34* transcript levels and their sensitivity to *A. brassicicola* inoculation. The responses of the accessions to *A. brassicicola* fell into two categories. Consistent with the results of a previous report (31), the susceptible group included Dijon-G, C24, Aua, RLD-1, Col-0, and Cvi (Fig. 7 *A* and *B*). Contrary to the results of the previous report (31), accessions No-0 and Be-0 were also susceptible to *A. brassicicola* under our experimental conditions (Fig. 7 *A* and *B*). The more resistant group included the remaining accessions.

Four of the seven susceptible accessions, No-0, Aua, RLD-1, and Be-0, expressed *AtABCG34* at similar or lower levels than did Col-0 (Fig. 7*C*). The three remaining susceptible accessions, Dijon-G, C24, and Cvi, expressed *AtABCG34* at five- to sixfold higher levels than did Col-0. By contrast, three of the four more resistant accessions, Kendallville, Ksk-1, and Mh, expressed *AtABCG34* at four- to 41-fold higher levels than did Col-0. The *AtABCG34* overexpression lines we generated fell into the more resistant group and expressed *AtABCG34* at 14- to 33-fold higher levels than did Col-0. Among the more resistant accessions, Tul-0 was the only accession that expressed *AtABCG34* at a level comparable to Col-0.

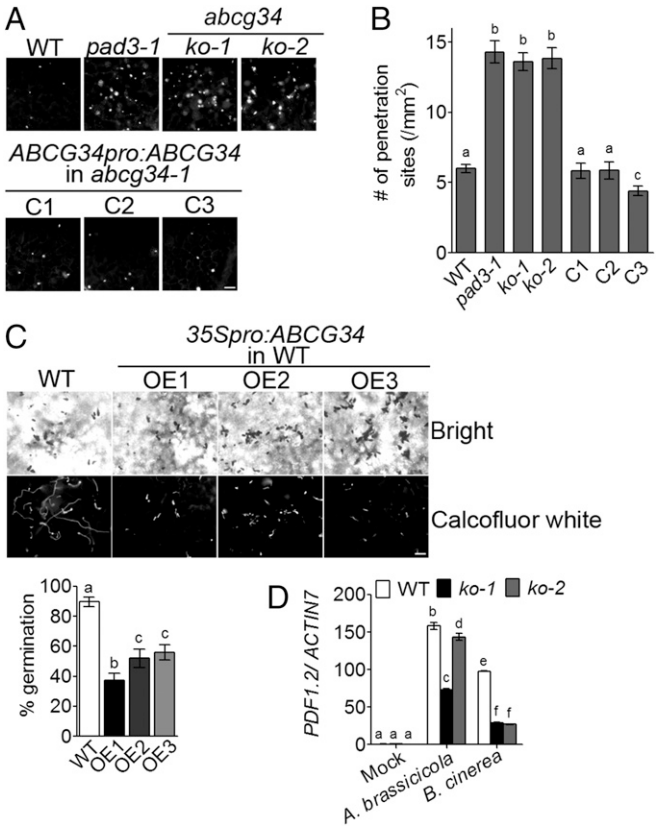

Fig. 6. AtABCG34 is required for preinvasion resistance to *A. brassicicola*. (*A* and *B*) Penetration sites in the leaves of various *A. thaliana* lines infected with *A. brassicicola*. (*A*) Callose deposited at the penetration sites was stained with aniline blue at 24 hpi. (Scale bar, 50 μm.) (*B*) The number of penetration sites was counted. Data represent mean values (±SE) of three independent experiments with at least 10 leaves per genotype in each experiment. Different lowercase letters indicate that the means are significantly different between genotypes (Tukey's HSD test, $P < 0.01$; $n = 3$). (*C*, *Upper*) Bright-field (*Upper Row*) and Calcofluor white fluorescent (*Lower Row*) microscopy images of *A. brassicicola* conidia and hyphae. (Scale bars, 50 μm.) (*Lower*) Percent germinated *A. brassicicola* conidia on the leaves of wild-type and AtABCG34-overexpressing plants at 24 hpi ($n = 15$). (*D*) Transcript levels of *AtPDF1.2* after *A. brassicicola* or *B. cinerea* infection in wild-type plants and *atabcg34* mutants. The graphs in *C*, *Lower* and *D* represent mean values (±SE) of three replicates ($n = 3$). Different lowercase letters indicate that the means are significantly different between the genotypes (Tukey's HSD test, $P < 0.05$).

To quantify the relationship between *AtABCG34* expression level and pathogen growth in different accessions and overexpression lines, we performed regression analysis. The coefficient of correlation was −0.27 when only the 12 accessions were included in the analysis (Fig. 7*D*), indicating a weak negative correlation between pathogen growth and *AtABCG34* expression levels in the accessions tested. However, the coefficient of correlation changed to −0.54 when three overexpression lines were included together with the 12 accessions (Fig. 7*E*), indicating a moderate negative correlation between pathogen growth and expression levels of *AtABCG34*.

Discussion

AtABCG34 Is Important for Defense Against Necrotrophic Fungi. In this study, we identified AtABCG34 as a strong factor conferring tolerance to the antifungal diterpene sclareol (Fig. 1 and Fig. S2)

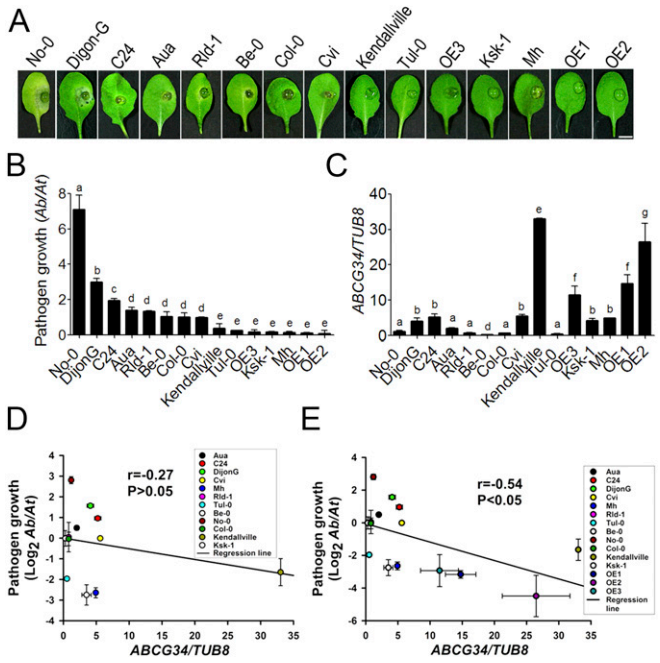

Fig. 7. *A. brassicicola* growth and *AtABCG34* expression levels in different accessions and *AtABCG34*-overexpressing lines of *Arabidopsis*. (*A*) Disease symptoms in detached leaves. Photographs were taken at 5 dpi with *A. brassicicola* (5×10^5 spores/mL). (Scale bar, 5 mm.) (*B*) Growth of *A. brassicicola*, as determined by amplification of the *A. brassicicola cutinase* A (*Ab*) and the *A. thaliana* α *shaggy kinase* (*At*) genes by qPCR. The graph represents mean values (±SE) from three biological replicates with 27 lesions from 15 different plants ($n = 3$). (*C*) *AtABCG34* transcript levels in leaves of 3- to 4-wk-old plants under control conditions. The graph represents mean values (±SE) from three biological replicates using qRT-PCR. Different lowercase letters in *B* and *C* indicate that the means are significantly different between the accessions (Tukey's HSD test, $P < 0.05$; $n = 3$). (*D* and *E*) Regression analysis for the correlation between *AtABCG34* expression (mean ± SE) and *A. brassicicola* growth (logarithmic transformed geometric mean ± SE) in 12 different accessions (*D*) and in 12 different accessions and three overexpression lines (OE1–OE3) (*E*).

and hence as a potential player in pathogen defense. We report three lines of evidence supporting the role of AtABCG34 in defense against necrotrophic fungal pathogens. First, *atabcg34* mutants exhibited hypersensitivity to the necrotrophic fungi *A. brassicicola* (Fig. 2) and *B. cinerea* (Fig. S4*A*). Second, *AtABCG34* expression was induced by *A. brassicicola* (Fig. 3 *C*, *G*, and *H*) and *B. cinerea* (Fig. S5) infection in a time-dependent manner. Third, *AtABCG34* expression was induced substantially by the application of MeJA (Fig. 3*A*) and only slightly by SA (Fig. 3*B*). The induction of *AtABCG34* by MeJA and necrotrophic fungal pathogens is similar to that observed for the NpPDR1 and NtPDR1 transporters, which secrete antifungal molecules in response to pathogen infection (4). MeJA was reported to be important for resistance to necrotrophic pathogens rather than biotrophic pathogens (32). Moreover, jasmonic acid (JA), but not SA, is necessary for the resistance to *A. brassicicola*, as evidenced by the reduced tolerance of a JA-signaling mutant, *coi1*, to the pathogen and the similar tolerance levels for the pathogen of the SA-signaling mutant *npr1*, SA-deficient *NahG*-expressing plants, and the wild-type plants, respectively (32). The pattern of *AtABCG34* induction (Fig. 3) suggests that AtABCG34 is involved in the defense against *A. brassicicola* through the JA-signaling pathway but not through the SA-signaling pathway. AtABCG34 does not seem to be involved in biotrophic pathogen resistance because (*i*) it was not induced significantly by SA, which is of major importance for biotrophic pathogen resistance (33), and (*ii*) the *atabcg34* mutants did not exhibit sensitivity to the biotrophic bacterial pathogen *Pst* DC3000 (Fig. S4*B*).

Possible Importance of AtABCG34 in Natural Habitat. In nature, multiple factors usually contribute to a phenotype. Thus, in an accession study, a very high correlation between the level of one factor and the phenotype is rare (34, 35). Consistently, in our results as well, there was only a weak negative correlation between *A. brassicicola* growth and *AtABCG34* expression levels (Fig. 7*D*). However, there was a significant, moderate negative correlation when overexpression lines were included together with the 12 accessions in the statistical analysis (Fig. 7*E*). Moreover, three of the four ecotypes resistant to *A. brassicicola* expressed *AtABCG34* at higher levels than did Col-0, whereas only three of the seven susceptible accessions did so (Fig. 7*C*). These results suggest that AtABCG34 contributes to the disease resistance in naturally occurring genetic variants. AtABCG34 may be one among many different factors contributing to *A. brassicicola* resistance, and only a subset of the accessions may have evolved this strategy. Other factors contributing to *A. brassicicola* resistance include other JA-response pathways (36), other secondary metabolites (such as phenolics), and a mechanism to tolerate the toxins secreted by the pathogen (31). Further studies, including analyses of additional accessions for resistance to fungal disease, are necessary to evaluate this hypothesis.

It is interesting that the expression level of *AtABCG34* was about 41 times higher in the Kendallville accession than in Col-0. Thus, in wild populations of *Arabidopsis*, there may be a wide range of expression levels of this gene. However, we do not expect that there would be many other accessions with even higher levels of expression of *AtABCG34* than the Kendallville ecotype, because the OE1 and OE3 lines expressed *AtABCG34* at lower levels than found in this accession but exhibited similar levels of resistance to *A. brassicicola* (Fig. 7*B*).

AtABCG34 Localization Before and After *A. brassicicola* Infection. AtABCG34 was localized at the outward-facing sides of the plasma membrane in epidermal cells of the leaves and roots (Fig. 3 *E* and *F*). Such polar localization of ABC transporters was reported previously for AtABCG32 (21), AtABCG36, and AtABCG37 (37). These transporters secrete compounds important for cuticle formation (21) or defense (13) or transport auxin precursor to the rhizosphere (38), respectively. The polar localization of AtABCG34 suggests that it secretes some compounds to the leaf surface. The mechanism of polar localization of AtABCG34 might resemble that of AtABCG36, another ABCG subfamily member involved in pathogen defense [i.e., polar secretion, constitutive endocytic recycling, and restricted lateral diffusion (39)].

AtABCG34 is highly induced by *A. brassicicola* infection (Fig. 3 *C* and *H*) and accumulates at the plasma membrane, as indicated by the increase in sGFP:ABCG34 fluorescence when plants are infected with the pathogen (Fig. 3*G*). Previous studies of AtABCG36/PEN3 and NbABCG1/2 showed that these transporters are preferentially localized at the pathogen penetration sites (5, 11). However, we did not observe such preferential accumulation of AtABCG34 at the penetration site. Rather, we observed its accumulation at broad areas surrounding the inoculation site of *A. brassicicola* (Fig. 3*G*) and *B. cinerea* (Fig. S5*B*). Interestingly, *A. brassicicola* infection also induced accumulation of sGFP:ABCG34 in dot-like structures that, to our knowledge, have not been reported for plant transporters during pathogen infection. Further studies are needed to decipher the formation and function of these dot-like structures.

AtABCG34 Most Likely Transports Camalexin. Our data described above indicate that AtABCG34 is involved in transporting secondary metabolites to the leaf surface to inhibit the growth of

necrotrophic pathogens. Initially, we selected AtABCG34 based on a screen for hypersensitivity to sclareol, a diterpene alcohol. However, based on several independent lines of evidence, we propose that the secondary metabolites that AtABCG34 transports include an indole alkaloid, camalexin (Fig. 8). First, surface camalexin in the rosette leaves was significantly reduced in *atabcg34* mutants (Fig. 4*A* and Fig. S6*D*), whereas the surface camalexin levels were increased in the AtABCG34-overexpressing lines (Fig. 4*A*). Second, expression of sGFP:ABCG34 in BY2 cells improved resistance to a toxic concentration of camalexin (Fig. 5 *B*–*D*), suggesting that AtABCG34 mediates the removal of camalexin from the BY2 cells. Third, when treated with exogenous camalexin, *atabcg34* mutants exhibited high levels of cell death, but the *atpad3-1* mutant did not (Fig. 5*A*), most likely because the functional AtABCG34 in the *atpad3-1* mutant plant cells was able to secrete camalexin from the cells. By contrast, there was no difference in the cell-death responses of the *atpad3-1* and *atabcg34* mutants to *A. brassicicola* treatment, indicating that both camalexin synthesis and transport are necessary for resistance against *A. brassicicola* infection. Fourth, the frequency of *A. brassicicola* penetration in the *atpad3-1* mutant was similar to that in the *atabcg34* mutants (Fig. 6 *A* and *B*). This result is consistent with our explanation that the two proteins function in the same pathway of defense against the pathogen: That PAD3 catalyzes the biosynthesis of camalexin, whereas AtABCG34 mediates transport of camalexin. Fifth, both AtABCG34 (Fig. 3*G* and Fig. S5*B*) and the camalexin biosynthesis genes (40) are induced around the *A. brassicicola* and *B. cinerea* infection site. By contrast, we did not obtain any clear evidence that the transporter transports surface-coating material (Fig. S6*A*), nor were there any clear differences in the levels of phenolics (in plants infected by *B. cinerea*) or glucosinolates (in plants infected by *A. brassicicola*) between the *atabcg34* and wild-type plants (Fig. S6 *B* and *C*). AtABCG34 might transport multiple substrates, such as an indole alkaloid camalexin and some diterpene alcohols similar to sclareol produced by *A. thaliana*. Such transport of multiple substrates would not be unusual, because a single ABCG transporter can transport many chemically unrelated substrates (41, 42), and ABCG transporters have a broad range of substrates, including alkaloids, terpenoids, various hormones, and lipids (41).

In addition, a comparison of our results with some previous reports supports the involvement of AtABCG34 in camalexin transport. Similar to AtABCG34, camalexin biosynthesis is induced by necrotrophic fungal pathogens (43). AtABCG34 is induced in response to JA (Fig. 3*A*), and JA-signaling components are involved in the biosynthesis of camalexin (25). Interestingly, a full-size ABCG transporter, BcatrB, in *B. cinerea* is necessary for the export of camalexin (44). This transporter is a critical virulence factor, as evidenced by the failure of a *BcatrB*-knockout mutant to infect *A. thaliana*. Thus, there may have been an evolutionary arms race between plants and the pathogen to develop camalexin transporters; plants developed ABC transporters to secrete camalexin, and fungal pathogens developed similar ABC transporters to export camalexin from their cytosol. Evolutionary studies on these transporters may lead to interesting findings on coevolution.

We attempted to conduct camalexin transport assays using BY2 cells. However, we did not find any conditions that allowed time-dependent loading of camalexin into cells. Similar difficulties in carrying out transport assays were reported for sclareol in BY2 cells (2). Direct transport assays of these secondary metabolites await further understanding of the chemical nature and permeability of the chemicals through lipid membranes. Nonetheless, our results strongly suggest that AtABCG34 has a critical role in secreting camalexin to the surface of the plant, where it inhibits invasion of *A. brassicicola*.

Because the level of surface camalexin was reduced to half that in the wild-type plants, we propose that other mechanisms, such as diffusion, or other transporters, such as ABC transporters, mediate the secretion of the remaining half of camalexin to the leaf surface. The only other ABCG member that has been reported to affect camalexin levels is AtABCG36; an increase in total camalexin content was observed in the *pdr8*/*pen3*/*abcg36* mutant in response to powdery mildew fungal infection (45). However, it is unclear whether the *pdr8* mutant has increased levels of surface camalexin, and the response of this mutant to *A. brassicicola* or *B. cinerea* has not been tested. Thus, whether there are additional ABCG transporters for camalexin remains to be determined.

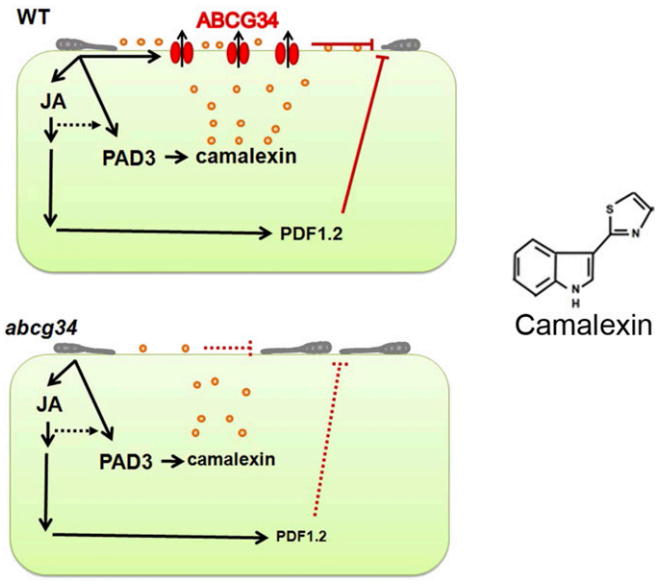

Fig. 8. Working model for the function of AtABCG34. Inoculation of *A. thaliana* leaves with *A. brassicicola* induces the expression of *AtABCG34*, the camalexin biosynthesis gene *PAD3*, and JA-signaling genes. JA also induces the expression of *AtABCG34* and *AtPDF1.2*. (*Upper Left*) AtABCG34-mediated secretion of camalexin to the surface inhibits *A. brassicicola* growth in wild-type plants (solid red lines). (*Lower Left*) Reduced camalexin secretion and *AtPDF1.2* expression (small font) allow pathogen growth in the *atabcg34* mutant (dotted red lines). Orange circles represent camalexin. (*Right*) The chemical structure of camalexin.

AtABCG34 Functions at the Preinvasion Stage. Some accessions of *Arabidopsis* exhibit an incompatible interaction with *A. brassicicola* and have evolved two layers of defense: pre- and postinvasion defense (46). Preinvasion defense culminates when the pathogen tries to penetrate the plant cell. Four of our findings suggest that AtABCG34 functions at the preinvasion step of defense. First, the level of camalexin was reduced in *atabcg34* mutants compared with wild-type plants (Fig. 4 *A* and *B* and Fig. S6*D*). Camalexin, a major phytoalexin in *A. thaliana*, is known to be important for preinvasion resistance against powdery mildew, and *atpad3-1*, a camalexin-deficient mutant, is defective in the preinvasion resistance to both powdery mildew (47) and *A. brassicicola* (33). Second, *A. brassicicola* conidia germination was significantly reduced in the AtABCG34-overexpressing lines (Fig. 6*C*), which had higher levels of surface camalexin (Fig. 4*A*). Inhibition of conidia germination on the plant surface is most likely caused by the higher level of camalexin secreted by AtABCG34. Third, *atabcg34* mutants exhibited higher penetration frequency than did the wild-type plants, and wild-type levels of penetration were restored in the complementation lines (Fig. 6 *A* and *B*). Furthermore, the *atpad3-1* mutant also exhibited high penetration frequency similar to that of the *atabcg34* mutants. In

general, mutants compromised in preinvasion defense exhibit high penetration frequency (marked by callose deposition) at the inoculation site (29, 48). Fourth, the expression levels of *AtPDF1.2*, a JA- and *A. brassicicola*-responsive gene, were significantly reduced in *atabcg34* mutants compared with the wild-type plants (Fig. 6*D*). *AtPDF1.2* is induced in response to necrotrophic fungal pathogens and JA (49), similar to *AtABCG34*, and constitutive expression of *PDF1.2* enhances preinvasion resistance (30). These results indicate that AtABCG34 has an important function in preinvasion resistance.

Other ABC transporters important for resistance at the preinvasion stage include NtPDR1 and NpPDR1, which transport sclareol (2, 3), an important factor for preinvasion resistance (5). Recently, NbABCG1 and NbABCG2 were reported to be important for both pre- and postinvasion resistance in *N. benthamiana* (5).

Application Potentials of AtABCG34. Our data revealed that AtABCG34 is an important factor required for defense against the necrotrophic fungal pathogens *A. brassicicola* and *B. cinerea* and that AtABCG34 functions by secreting camalexin to the surface. *A. brassicicola* infection results in dark leaf spots on most *Brassica* species, including economically important oilseed crops (50). Infection by *A. brassicicola* considerably reduces the quality and quantity of harvested *Brassica* crops (51), resulting in annual yield losses of 15–70% (51). Interestingly, overexpression of AtABCG34 in *A. thaliana* enhanced the surface camalexin content (Fig. 4*A*) and resistance to *A. brassicicola* (Fig. 4*C*). We predict that high levels of *AtABCG34* expression in economically important *Brassica* species, such as *Brassica napus* and *Brassica oleracea*, will be associated with reduced disease severity and yield loss following *A. brassicicola* infection because of the increased secretion of camalexin to the plant's surface. Such a goal may be attained by genetic approaches or by screening and selecting for accessions of *B. napus* and *B. oleracea* that have naturally high levels of expression of the *ABCG34* ortholog.

Materials and Methods

Plant Materials and Growth Conditions. *A. thaliana* (L.) Heynh. ecotype Col-0 wild-type and transgenic plants were grown on 1/2MS agar plates with 1% sucrose in the presence or absence of sclareol (65 μM) for 2–3 wk at a 16/8 h light/dark, 22/18 °C cycle. For long-term experiments, plants were transferred to soil and grown in a controlled growth chamber (16/8 h light/dark; 22/18 °C). For pathogen infection and camalexin analysis, 3- to 4-wk-old plants were used. For accessions analysis, Kendallville (CS76344), Bensheim (Be-0- CS76345), Aua/Rhon (CS900), Cape Verde (Cvi-CS902), Muehlen (Mh-CS904), C24 (CS906), Dijon-G (CS910), Col-0 (CS1092), Ksk-1 (CS1634), Rld-1 (CS76588), Tul-0 (CS76618), and No-0 (CS28564) strains were used.

Fungal Culture and Disease Assays. *B. cinerea* was grown on 2× V8 agar [36% V8 juice (Campbell's), 0.2% $CaCO_3$, and 2% Bacto-agar] at 25 °C for 1–2 wk, and spores were resuspended in 1% Sabouraud maltose broth buffer (SMBB; Difco). *A. brassicicola* strain KACC40036 was grown on potato dextrose agar and was resuspended in distilled water for plant inoculation (52). To examine gene-expression patterns, whole *A. thaliana* plants were inoculated with *B. cinerea* or *A. brassicicola* by spraying the plants with a spore suspension (5×10^5 spores/mL) in SMBB or distilled water, respectively. For the disease assay, 8 μL of the spore suspension (5×10^5 spores/mL) was dropped onto detached leaves. Inoculated leaves were kept under high humidity until 5 dpi. The *B. cinerea* spore population was counted as described previously (23). *A. brassicicola* growth was quantified as follows: leaf disks were collected from the infection area at 5 dpi, using a No. 2 cork borer. The genomic DNA was extracted, and qPCR was performed as described previously (53). To estimate the growth of *A. brassicicola cutinase A* (*ABU03393*), DNA was amplified using primers listed in Table S1. The value was normalized by amplifying genomic DNA of *A. thaliana α-Shaggy kinase* (*At5g26751*) using iASK1 and iASK2 primers (Table S1). Standard curves were prepared using genomic DNA extracted from the *A. thaliana* leaf disks and *A. brassicicola* grown on potato dextrose agar plates. For the intact-plant assay, 10 μL of spore suspension (5×10^5 spores/mL) in distilled water was dropped on the fully expanded leaves of 4-wk-old plants.

Camalexin Level Assay. Four-week-old plants were sprayed with spore suspension (5×10^5 spores/mL) of *A. brassicicola*, and whole rosettes were collected at the indicated time points (Fig. 4 *A* and *B* and Fig. S6*D*). Total camalexin was extracted with hot methanol and chloroform, and surface camalexin was extracted with dichloromethane, using established protocols (54, 55) with slight modifications. To extract surface camalexin, rosette leaves of *A. thaliana* were gently rotated in dichloromethane for 30 s. Extracted samples were loaded onto a TLC plate and were separated, and the camalexin band was visualized by its blue fluorescence under an UV lamp (365 nm). The silica containing camalexin was scraped off the plate, and camalexin was extracted into 500 μL of methanol. The emission at 385 nm after excitation at 315 nm was measured to quantify the camalexin in a 96-well black microplate (Greiner Bio-One) with a Tecan fluorometer (M200PRO). The camalexin concentration was calculated by comparison with a standard curve obtained using commercially available camalexin purchased from Glixx Laboratories.

Camalexin Toxicity Assay. Three-week-old plants were treated with 1% DMSO (solvent control treatment), 1 mg/mL camalexin, or 5×10^5 spores/mL of *A. brassicicola* (positive control). Evans blue staining was performed 24 h after treatment as described previously (56). Briefly, 0.1% Evans blue solution (wt/vol) was vacuum infiltrated (25 mmHg for 5 min, followed by a 5-min hold and subsequent slow release), and the leaves were stained for 8 h at room temperature. After staining, samples were washed with a PBS solution containing 0.05% (vol/vol) Tween-20 until the washing solution became clear.

For BY2 cells, the 6-d-old culture was treated with 250 μM camalexin for 30 min at 25 °C in darkness (24). The cells were washed with water and harvested by centrifugation at 13,800 × *g* for 5 min at room temperature. To analyze cell death, cells were stained with 0.05% Evans blue for 15 min at 25 °C and then were washed three times with water (56). Evans blue stain was extracted from the cells with 50% methanol+1% SDS for 60 min at 60 °C, and the blue color was quantified by measuring absorbance at 595 nm and normalized by OD at 600 nm. Cell death caused by boiling, used as a positive control, was set to 100%, and relative cell death caused by either DMSO or camalexin treatment was analyzed. For cell growth analysis, a 3-d-old culture was treated with either 0.01% DMSO (solvent control) or camalexin (50 μM), and OD at 600 nm was measured 3 d after camalexin treatment using a spectrophotometer.

Callose Staining. Callose staining was performed as described previously (12). Briefly, 3- to 4-wk-old plants were treated with *A. brassicicola* solution (5×10^5 spores/mL). Leaf disks from the inoculation sites were collected 24 hpi and fixed in ethanol:acetic acid (3:1) by brief vacuum infiltration (at 25 mmHg for 5 min, followed by a 5-min hold and subsequent slow release) and then were destained by gentle rotation until the disks became translucent, washed with 150 mM K_2HPO_4 for 30 min, and stained with aniline blue (1%) staining solution for 2 h on a shaker. Stained disks were observed with a Zeiss fluorescence microscope (Axioskop 2 MOT) using the DAPI channel after mounting with 50% glycerol.

Regression Analysis Between *AtABCG34* Expression and Pathogen Growth in Natural Accessions. The expression levels of *AtABCG34* and pathogen growth in different ecotypes were analyzed as mentioned above using sets of primers listed in Table S1. The *AtABCG34* sequences of all ecotypes tested contained fragments that precisely matched the sequences of the primers used. The tubulin 8 sequences differed from those of the primers (both forward and reverse) by 1 bp in two ecotypes, Kendallville and RLD-1. However, the transcript levels of tubulin 8 in these two ecotypes were similar to those of other the ecotypes evaluated.

The Ksk-1 and Bensheim ecotypes have not been sequenced. Thus, we sequenced parts of the coding regions of *AtTubulin 8* and *AtABCG34*. No differences were observed in the regions corresponding to the *AtABCG34* primer sequences in either of the two ecotypes. One base pair change was detected in the center of both the forward and reverse primers of *AtTubulin 8* in Bensheim. The tubulin 8 sequence of Ksk-1 differed at 3 bp of the forward primer. Thus, we designed a different forward primer (listed in Table S1) to compare the transcript levels of tubulin 8 in Ksk-1 and Col-0.

Regression analysis between *AtABCG34* expression and pathogen growth was performed by comparing the Pearson's correlation coefficient between average data of *AtABCG34* expression and pathogen growth with 10,000 randomly permuted datasets from all 12 accessions either including or excluding three overexpression (OE1–OE3) lines. Logarithmic values of relative copy numbers of *A. brassicicola cutinase A* were used for pathogen growth.

For other methods, please see *SI Materials and Methods*.

ACKNOWLEDGMENTS. We thank Professor Jane Glazebrook for kindly providing camalexin and Dr. C. Douglas Grubb for measuring glucosinolates. This work was supported by National Research Foundation of Korea (NRF) Grant NRF-2015R1A2A1A01004294 (to Y.L.) and by NRF Grant R1A2A2A01002476 (to K.-H.P.). The NRF is funded by the Ministry of Science, ICT and Future Planning of the Korean Government.

1. Srikantaramas S, Yamazaki M, Saito K (2008) Mechanisms of resistance to self-produced toxic secondary metabolites in plants. *Phytochem Rev* 7:467–477.
2. Crouzet J, et al. (2013) NtPDR1, a plasma membrane ABC transporter from *Nicotiana tabacum*, is involved in diterpene transport. *Plant Mol Biol* 82:181–192.
3. Jasiński M, et al. (2001) A plant plasma membrane ATP binding cassette-type transporter is involved in antifungal terpenoid secretion. *Plant Cell* 13:1095–1107.
4. Stukkens Y, et al. (2005) NpPDR1, a pleiotropic drug resistance-type ATP-binding cassette transporter from *Nicotiana plumbaginifolia*, plays a major role in plant pathogen defense. *Plant Physiol* 139:341–352.
5. Shibata Y, et al. (2016) The Full-size ABCG transporters Nb-ABCG1 and Nb-ABCG2 function in pre- and post-invasion defense against *Phytophthora infestans* in *Nicotiana benthamiana*. *Plant Cell* 28:1163–1181.
6. Bienert MD, et al. (2012) A pleiotropic drug resistance transporter in *Nicotiana tabacum* is involved in defense against the herbivore *Manduca sexta*. *Plant J* 72: 745–757.
7. Sasse J, et al. (2016) *Petunia hybrida* PDR2 is involved in herbivore defense by controlling steroidal contents in trichomes. *Plant Cell Environ* 39:2725–2739.
8. Yu F, De Luca V (2013) ATP-binding cassette transporter controls leaf surface secretion of anticancer drug components in *Catharanthus roseus*. *Proc Natl Acad Sci USA* 110: 15830–15835.
9. Krattinger SG, et al. (2009) A putative ABC transporter confers durable resistance to multiple fungal pathogens in wheat. *Science* 323:1360–1363.
10. Krattinger SG, et al. (2016) The wheat durable, multipathogen resistance gene Lr34 confers partial blast resistance in rice. *Plant Biotechnol J* 14:1261–1268.
11. Underwood W, Somerville SC (2013) Perception of conserved pathogen elicitors at the plasma membrane leads to relocalization of the *Arabidopsis* PEN3 transporter. *Proc Natl Acad Sci USA* 110:12492–12497.
12. Clay NK, Adio AM, Denoux C, Jander G, Ausubel FM (2009) Glucosinolate metabolites required for an *Arabidopsis* innate immune response. *Science* 323:95–101.
13. Stein M, et al. (2006) Arabidopsis PEN3/PDR8, an ATP binding cassette transporter, contributes to nonhost resistance to inappropriate pathogens that enter by direct penetration. *Plant Cell* 18:731–746.
14. Lu X, et al. (2015) Mutant allele-specific uncoupling of PEN3 functions reveals engagement of the ABC25 transporter in distinct tryptophan metabolic pathways. *Plant Physiol* 168:814–827.
15. Campbell EJ, et al. (2003) Pathogen-responsive expression of a putative ATP-binding cassette transporter gene conferring resistance to the diterpenoid sclareol is regulated by multiple defense signaling pathways in *Arabidopsis*. *Plant Physiol* 133: 1272–1284.
16. Kang J, et al. (2011) Plant ABC transporters. *Arabidopsis Book* 9:e0153.
17. Ji H, et al. (2014) ATP-dependent binding cassette transporter G family member 16 increases plant tolerance to abscisic acid and assists in basal resistance against *Pseudomonas syringae* DC3000. *Plant Physiol* 166:879–888.
18. Yazaki K (2006) ABC transporters involved in the transport of plant secondary metabolites. *FEBS Lett* 580:1183–1191.
19. Bailey JA, Garter GA, Burden RS, Wain RL (1975) Control of rust diseases by diterpenes from *Nicotiana glutinosa*. *Nature* 255:328–329.
20. Kennedy BS, et al. (1992) Leaf surface chemicals from*Nicotiana* affecting germination of *Peronospora tabacina* (adam) sporangia. *J Chem Ecol* 18:1467–1479.
21. Bessire M, et al. (2011) A member of the PLEIOTROPIC DRUG RESISTANCE family of ATP binding cassette transporters is required for the formation of a functional cuticle in *Arabidopsis*. *Plant Cell* 23:1958–1970.
22. Fabre G, et al. (2016) The ABCG transporter PEC1/ABCG32 is required for the formation of the developing leaf cuticle in *Arabidopsis*. *New Phytol* 209:192–201.
23. van Wees SC, Chang HS, Zhu T, Glazebrook J (2003) Characterization of the early response of *Arabidopsis* to *Alternaria brassicicola* infection using expression profiling. *Plant Physiol* 132:606–617.
24. Rogers EE, Glazebrook J, Ausubel FM (1996) Mode of action of the *Arabidopsis thaliana* phytoalexin camalexin and its role in *Arabidopsis*-pathogen interactions. *Mol Plant Microbe Interact* 9:748–757.
25. Zhou N, Tootle TL, Glazebrook J (1999) *Arabidopsis PAD3*, a gene required for camalexin biosynthesis, encodes a putative cytochrome P450 monooxygenase. *Plant Cell* 11:2419–2428.
26. Lawrence CB, et al. (2008) At death's door: Alternaria pathogenicity mechanisms. *Plant Pathol J* 24:101–111.
27. Cho Y, Ohm RA, Grigoriev IV, Srivastava A (2013) Fungal-specific transcription factor AbPf2 activates pathogenicity in *Alternaria brassicicola*. *Plant J* 75:498–514.
28. Flors V, et al. (2008) Interplay between JA, SA and ABA signalling during basal and induced resistance against *Pseudomonas syringae* and *Alternaria brassicicola*. *Plant J* 54:81–92.
29. Lipka V, et al. (2005) Pre- and postinvasion defenses both contribute to nonhost resistance in *Arabidopsis*. *Science* 310:1180–1183.
30. Hiruma K, et al. (2011) *Arabidopsis* ENHANCED DISEASE RESISTANCE 1 is required for pathogen-induced expression of plant defensins in nonhost resistance, and acts through interference of MYC2-mediated repressor function. *Plant J* 67:980–992.
31. Kagan IA, Hammerschmidt R (2002) *Arabidopsis* ecotype variability in camalexin production and reaction to infection by *Alternaria brassicicola*. *J Chem Ecol* 28: 2121–2140.
32. Thomma BPHJ, et al. (1998) Separate jasmonate-dependent and salicylate-dependent defense-response pathways in *Arabidopsis* are essential for resistance to distinct microbial pathogens. *Proc Natl Acad Sci USA* 95:15107–15111.
33. Glazebrook J (2005) Contrasting mechanisms of defense against biotrophic and necrotrophic pathogens. *Annu Rev Phytopathol* 43:205–227.
34. Stein RJ, Waters BM (2012) Use of natural variation reveals core genes in the transcriptome of iron-deficient *Arabidopsis thaliana* roots. *J Exp Bot* 63:1039–1055.
35. Barah P, et al. (2013) Genome-scale cold stress response regulatory networks in ten *Arabidopsis thaliana* ecotypes. *BMC Genomics* 14:722.
36. Cramer RA, Lawrence CB (2004) Identification of *Alternaria brassicicola* genes expressed *in planta* during pathogenesis of *Arabidopsis thaliana*. *Fungal Genet Biol* 41: 115–128.
37. Langowski L, Růzicka K, Naramoto S, Kleine-Vehn J, Friml J (2010) Trafficking to the outer polar domain defines the root-soil interface. *Curr Biol* 20:904–908.
38. Ružicka K, et al. (2010) *Arabidopsis* PIS1 encodes the ABCG37 transporter of auxinic compounds including the auxin precursor indole-3-butyric acid. *Proc Natl Acad Sci USA* 107:10749–10753.
39. Łangowski Ł, et al. (2016) Cellular mechanisms for cargo delivery and polarity maintenance at different polar domains in plant cells. *Cell Discov* 2:16018.
40. Glawischnig E, Hansen BG, Olsen CE, Halkier BA (2004) Camalexin is synthesized from indole-3-acetaldoxime, a key branching point between primary and secondary metabolism in *Arabidopsis*. *Proc Natl Acad Sci USA* 101:8245–8250.
41. Crouzet J, Trombik T, Fraysse AS, Boutry M (2006) Organization and function of the plant pleiotropic drug resistance ABC transporter family. *FEBS Lett* 580:1123–1130.
42. Jungwirth H, Kuchler K (2006) Yeast ABC transporters– A tale of sex, stress, drugs and aging. *FEBS Lett* 580:1131–1138.
43. Zhao J, Last RL (1996) Coordinate regulation of the tryptophan biosynthetic pathway and indolic phytoalexin accumulation in *Arabidopsis*. *Plant Cell* 8:2235–2244.
44. Stefanato FL, et al. (2009) The ABC transporter BcatrB from *Botrytis cinerea* exports camalexin and is a virulence factor on *Arabidopsis thaliana*. *Plant J* 58:499–510.
45. Bednarek P, et al. (2009) A glucosinolate metabolism pathway in living plant cells mediates broad-spectrum antifungal defense. *Science* 323:101–106.
46. Mysore KS, Ryu C-M (2004) Nonhost resistance: How much do we know? *Trends Plant Sci* 9:97–104.
47. Consonni C, et al. (2010) Tryptophan-derived metabolites are required for antifungal defense in the *Arabidopsis mlo2* mutant. *Plant Physiol* 152:1544–1561.
48. Egusa M, Miwa T, Kaminaka H, Takano Y, Kodama M (2013) Nonhost resistance of *Arabidopsis thaliana* against *Alternaria alternata* involves both pre- and postinvasive defenses but is collapsed by AAL-toxin in the absence of *LOH2*. *Phytopathology* 103: 733–740.
49. Lazniewska J, Macioszek VK, Lawrence CB, Kononowicz AK (2010) Fight to the death: *Arabidopsis thaliana* defense response to fungal necrotrophic pathogens. *Acta Physiol Plant* 32:1–10.
50. Nowicki M, Nowakowska M, Niezgoda A, Kozik E (2012) Alternaria black spot of crucifers: Symptoms, importance of disease, and perspectives of resistance breeding. *Vegetable Crops Research Bulletin* (Versita, Warsaw), 10.2478/v10032-012-0001-6.
51. Kumar D, et al. (2014) Alternaria blight of oilseed Brassicas: A comprehensive. *Afr J Microbiol Res* 8:2816–2829.
52. Choi J, et al. (2010) The cytokinin-activated transcription factor ARR2 promotes plant immunity via TGA3/NPR1-dependent salicylic acid signaling in *Arabidopsis*. *Dev Cell* 19:284–295.
53. Gachon C, Saindrenan P (2004) Real-time PCR monitoring of fungal development in *Arabidopsis thaliana* infected by *Alternaria brassicicola* and *Botrytis cinerea*. *Plant Physiol Biochem* 42:367–371.
54. Glazebrook J, Ausubel FM (1994) Isolation of phytoalexin-deficient mutants of *Arabidopsis thaliana* and characterization of their interactions with bacterial pathogens. *Proc Natl Acad Sci USA* 91:8955–8959.
55. Savatin DV, Bisceglia NG, Gravino M, Fabbri C, Pontiggia D, Mattei B (2015) Camalexin quantification in leaves infected with *B. cinerea*. *Bio Protoc* 5:e1379.
56. Ohno R, et al. (2011) Cryptogein-induced cell cycle arrest at G2 phase is associated with inhibition of cyclin-dependent kinases, suppression of expression of cell cycle-related genes and protein degradation in synchronized tobacco BY-2 cells. *Plant Cell Physiol* 52:922–932.
57. Mengiste T, Chen X, Salmeron JM, Dietrich RA (2003) The *BOTRYTIS SUSCEPTIBLE1* gene encodes an R2R3MYB transcription factor protein that is required for biotic and abiotic stress responses in *Arabidopsis*. *Plant Cell* 15:2551–2565.
58. Grubb CD, Gross HB, Chen DL, Abel S (2002) Identification of *Arabidopsis* mutants with altered glucosinolate profiles based on isothiocyanate bioactivity. *Plant Sci* 162: 143–152.